Line-of-Sight Path Following for Dubins Paths with Adaptive Sideslip Compensation of Drift Forces

Fossen, Thor Inge; Pettersen, Kristin Ytterstad; Galeazzi, Roberto

Published in:
IEEE Transactions on Control Systems Technology

Link to article, DOI:
10.1109/TCST.2014.2338354

Publication date:
2015

Document Version
Peer reviewed version

Line-of-Sight Path Following for Dubins Paths with Adaptive Sideslip Compensation of Drift Forces

Thor I. Fossen, Kristin Y. Pettersen, *Senior Members, IEEE,* and Roberto Galeazzi, *Member*

***Abstract*—We present a nonlinear adaptive path-following controller that compensates for drift forces through vehicle sideslip. Vehicle sideslip arises during path following when the vehicle is subject to drift forces caused by ocean currents, wind and waves. The proposed algorithm is motivated by a line-of-sight (LOS) guidance principle used by ancient navigators, which is here extended to path following of Dubins paths. The unknown sideslip angle is treated as a constant parameter, which is estimated using an adaptation law. The equilibrium points of the cross-track and parameter estimation errors are proven to be uniformly semiglobally exponentially stable (USGES). This guarantees that the estimated sideslip angle converges to its true value exponentially. The adaptive control law is in fact an integral LOS controller for path following since the parameter adaptation law provides integral action. The proposed guidance law is intended for maneuvering in the horizontal-plane at given speeds and typical applications are marine craft, autonomous underwater vehicles (AUVs), unmanned aerial vehicles (UAVs) as well as other vehicles and craft where the goal is to follow a predefined parametrized curve without time constraints. Two vehicle cases studies are included to verify the theoretical results.**

***Index Terms*—Adaptive control; path planning; kinematics; unmanned aerial vehicles, marine vehicles; land vehicles.**

I. Introduction

MARINE vessels, AUVs and UAVs rely heavily on guidance systems in order to accomplish desired motion control scenarios such as object tracking, path following, path tracking and path maneuvering; see Breivik et al. [4], Breivik and Fossen [5], and Yanushevsky [27] for instance. This paper considers aerial and marine vehicles exposed to wind, waves and currents. An overview of path-following methods for wheeled vehicles are found in Morin and Samson [23], while automatic guidance systems for farm vehicles are presented by Hao et al. [14], Lenain et al. [19] and references therein.

For ships and offshore platforms it is common to specify a two-dimensional (2-D) desired path parametrized by straight lines and circle segments (Dubins [10]). AUVs and UAVs operate in three dimensions. However, it is quite common to assume that altitude/depth is controlled independently such that the path-following objective is limited to motion control in the horizontal plane. For path-following applications in the horizontal plane, the control objective is to follow a predefined planar path without time information. Path-following methods for underactuated vehicles in the presence of large modeling parametric uncertainty using adaptive supervisory control that combines logic-based switching with Lyapunov-based techniques are discussed by Aguiar and Hespanha [1]. An alternative model-based approach for robust adaptive path following is proposed by Do et al. [9]. Planar path-following controllers for underactuated marine vehicles using polar-like kinematic models have been investigated by Aicardi et al. [2].

A popular and effective way to achieve convergence to the desired path is to implement a look-ahead LOS guidance law mimicking an experienced sailor (Healey and Lienhard [15]). The main advantages of a LOS guidance law are simplicity and a small computational footprint. In addition we show that strong stability properties such as USGES hold. LOS guidance laws can also be used together with commercial heading autopilot systems as shown in Figure 2. Complexity drastically increases if speed and heading are stabilized simultaneously, see Lapierre et al. [17] and Skjetne et al. [24] for instance. In this paper we assume that the vehicle's speed is measured and derive a new LOS guidance law for path following compensating for drift forces. This is based on the principle that underactuated vehicles can be stabilized by specifying a geometric and a dynamic task as defined by Skjetne et al. [24]. The geometric task is solved by using a guidance law for steering. However, the solution of the dynamic task (speed requirement) is not undertaken in our approach. Hence, the operator can control speed manually using the throttle.

A. Proportional LOS guidance

Guided LOS motion control of AUVs using sliding mode control for stabilizing the combined speed, steering and diving responses was first addressed by Healey and Lienhard [15]. The LOS guidance principle for straight-line path following of marine craft is discussed by Pettersen and Lefeber [21] and Fossen et al. [11]. An overview of the LOS guidance principles for marine craft are found in Fossen [12]. Similar techniques have been used for UAVs and missiles, see Yanushevsky [27] and Siouris [25].

Uniform global asymptotic stability (UGAS) and uniform local exponential stability (ULES) of the *proportional* LOS guidance law was first proven by Pettersen and Lefeber [21] in connnection with a simplified vehicle model. This is also referred to as *global κ-exponential stability* as defined by Sørdalen and Egeland [26]. This result was further extended to include the analysis of underactuated ship models by Børhaug and Pettersen [6], and Fredriksen and Pettersen [13]. Extensions to underactuated underwater vehicles are made by Børhaug and Pettersen [7].

T. I. Fossen and K. Y. Pettersen are with the Centre for Autonomous Marine Operations, Department of Engineering Cybernetics, Norwegian University of Science, Trondheim, Norway (e-mail: fossen@ieee.org, kyp@itk.ntnu.no).

R. Galeazzi is with the Department of Electrical Engineering, Technical University of Denmark, Kgs. Lyngby, Denmark (e-mail: rg@elektro.dtu.dk)

B. Proportional-integral LOS guidance

Despite the effectiveness and simplicity of *proportional* LOS guidance laws they have limitations when the vehicle is exposed to unknown *drift forces*, which are caused by waves, wind, ocean currents or other external disturbances. Underactuated vehicles do not have a direct control force in the sideways (sway) direction. Hence, convergence to a curved path under the influence of an unknown drift force is non-trivial. Using proportional guidance laws, such vehicles will exhibit large cross-track errors during path following and also in steady state. The offset depends on the path curvature as well as the direction and strength of the drift force. To overcome these difficulties it is necessary to modify the LOS guidance law to include integral action. This is referred to as *proportional-integral* (PI) guidance or *integral* LOS. This was introduced for ships in Børhaug et al. [8] where convergence to the desired straight-line path was proven. In particular, the integral LOS guidance law was proven global κ-exponential stable for straight-line path following at constant speed.

C. Main results

The main result of the paper is a nonlinear integral LOS guidance law based on adaptive control theory, which effectively compensates for constant and slowly varying drift forces due to waves, wind and ocean currents. The guidance law is derived for *Dubins paths*, *time-varying speed* and *time-varying look-ahead distance* under the assumption that no measurements of the environmental forces are available and that the sideslip angle is slowly varying for curved paths. In addition, the path must be $\mathcal{C}^1$ differentiable. The adaptive integral LOS guidance law has a very small computational footprint, which makes the proposed formula highly practical.

The new guidance law includes an integral term, which is structurally different from the well-established integral LOS algorithm of Børhaug et al. [8]. Lyapunov analysis is employed in order to prove USGES, while previous results only guarantee global κ-exponential stability. This is advantageous since USGES implicitly guarantees stronger convergence and robustness properties. For instance, it follows from Lemma 9.2 in Khalil [16] that the USGES property implies that we always can choose a region of attraction in which we have exponential convergence sufficiently large. Hence, we can always satisfy the condition for which the solution of the perturbed system will be uniformly bounded irrespective of the size of the perturbation. USGES thus provides stronger robustness properties than global κ-exponential stability.

D. Organization of the paper

The paper is organized as follows: In Section II the kinematic equations for LOS guidance systems are derived. Section III presents the adaptive LOS guidance law, while Section IV contains vehicle case studies verifying the theoretical results.

II. Kinematics

In the remaining of the paper, we consider a vehicle that is assigned to converge to a 2-D path specified by straight lines or curves, see Figure 1. 2-D paths are commonly used for guidance of surface vessels, while for aircraft and underwater vehicles we assume that the altitude/depth is controlled independently such that the path-following control problem is limited to motions in the horizontal plane. Without loss of generality, the presented method can be extended to 3-D guidance by following a similar approach as Lekkas and Fossen [18].

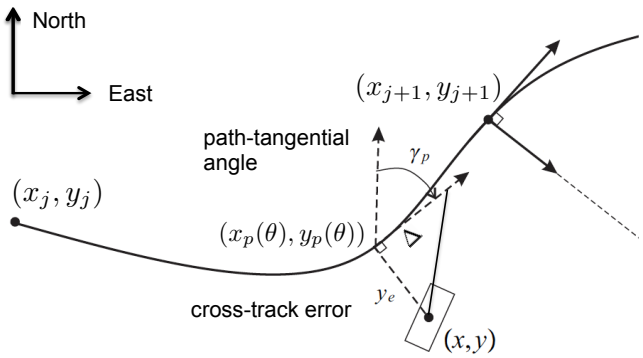

Fig. 1. LOS guidance geometry.

A. Cross-track error

A $\mathcal{C}^1$ parametrized path $(x_p(\theta), y_p(\theta))$, where $\theta \geq 0$ denotes the path variable, is assumed to go through a set of successive waypoints (x_j, y_j) for $j = 1, 2, ..., N_p$ as illustrated in Figure 1. For any point $(x_p(\theta), y_p(\theta))$ along the path, the path-tangential reference frame is rotated an angle[1]:

$$\gamma_p(\theta) = \text{atan2}\left(y_p'(\theta), x_p'(\theta)\right) \tag{1}$$

where $x_p'(\theta) = \partial x_p/\partial\theta$ and $y_p'(\theta) = \partial y_p/\partial\theta$. Notice that for a straight line $\gamma_p = \text{atan2}(y_{j+1} - y_j, x_{j+1} - x_j)$ is constant between the waypoints.

For a vehicle located at (x, y) the cross-track error is computed as the orthogonal distance to the path-tangential reference frame defined by the point $(x_p(\theta), y_p(\theta))$. Hence,

$$\begin{bmatrix} 0 \\ y_e \end{bmatrix} = \underbrace{\begin{bmatrix} \cos(\gamma_p(\theta)) & -\sin(\gamma_p(\theta)) \\ \sin(\gamma_p(\theta)) & \cos(\gamma_p(\theta)) \end{bmatrix}^\top}_{\mathbf{R}(\gamma_p(\theta))} \begin{bmatrix} x - x_p(\theta) \\ y - y_p(\theta) \end{bmatrix} \tag{2}$$

Moreover, the path-tangential reference frame is rotated an angle $\gamma_p(\theta)$ using the rotation matrix $\mathbf{R}(\gamma_p(\theta)) \in SO(2)$. Expanding (2) gives the path-normal line:

$$y - y_p(\theta) = -\frac{1}{\tan(\gamma_p(\theta))}(x - x_p(\theta)) \tag{3}$$

through $(x_p(\theta), y_p(\theta))$ and the cross-track error

$$y_e = -(x - x_p(\theta))\sin(\gamma_p(\theta)) + (y - y_p(\theta))\cos(\gamma_p(\theta)) \tag{4}$$

[1]The function $\text{atan2}(y, x)$ returns the angle between the positive x-axis of a plane and the point given by the coordinates (x, y) on it.

The path variable propagates according to (Fossen [12]):

$$\dot{\theta} = \frac{U}{\sqrt{x_p'(\theta)^2 + y_p'(\theta)^2}} > 0 \tag{5}$$

As pointed out by Samson [22] there may be infinite solutions of (3) if the path is a closed curve. In the following we will assume that the path is an open curve, that is the end point is different from the start point. Definition 1 guarantees that there is a unique solution for the cross-track error y_e obtained by minimizing $\dot{\theta}$. The unique solution of (4) is denoted $y_e(\theta^*)$ and is defined by:

Definition 1 (Uniqueness of solutions):

$$\theta^* := \arg\min_{\theta \geq 0} \left\{ \frac{U^2}{x_p'(\theta)^2 + y_p'(\theta)^2} \right\} \tag{6}$$

subject to

$$y - y_p(\theta) = -\frac{1}{\tan(\gamma_p(\theta))}(x - x_p(\theta)) \tag{7}$$

This is a nonlinear optimization problem, which can be solved numerically. However, for many paths θ^* can be found by computing all possible projection candidates θ_i $(i = 1, \ldots, M)$ given by (3) and choose the one closest to the previous θ^*-value.

B. Equations of motion

The kinematic equations expressed in terms of the *surge*, *sway* and *yaw* velocities u, v and r are (Fossen [12]):

$$\dot{x} = u\cos(\psi) - v\sin(\psi) \tag{8}$$

$$\dot{y} = u\sin(\psi) + v\cos(\psi) \tag{9}$$

$$\dot{\psi} = r \tag{10}$$

where ψ is the yaw angle. Time differentiation of (4) gives:

$$\begin{aligned} \dot{y}_e = &-(\dot{x} - \dot{x}_p(\theta^*))\sin(\gamma_p) + (\dot{y} - \dot{y}_p(\theta^*))\cos(\gamma_p) \\ &- [(x - x_p(\theta^*))\cos(\gamma_p) + (y - y_p(\theta^*))\sin(\gamma_p)]\,\dot{\gamma}_p \end{aligned} \tag{11}$$

The last bracket in (11) is zero because of (3) and

$$\dot{x}_p(\theta^*)\sin(\gamma_p) - \dot{y}_p(\theta^*)\cos(\gamma_p) = 0 \tag{12}$$

according to (1). Consequently, (8), (9) and (11) give:

$$\begin{aligned} \dot{y}_e &= -\dot{x}\sin(\gamma_p) + \dot{y}\cos(\gamma_p) \\ &= -(u\cos(\psi) - v\sin(\psi))\sin(\gamma_p) \\ &\quad + (u\sin(\psi) + v\cos(\psi))\cos(\gamma_p) \end{aligned} \tag{13}$$

This can be written in *amplitude-phase form*:

$$\dot{y}_e = U\sin(\psi - \gamma_p + \beta) \tag{14}$$

where the amplitude $U = \sqrt{u^2 + v^2} > 0$ and the phase $\beta = \text{atan2}(v, u)$ are recognized as the speed and sideslip angle, respectively. A vehicle exposed to drift forces (wind, waves and ocean currents) exhibits variations in the velocities u, v and r due to *Newton's second law*, which defines the kinetic equations of motion. The response can be observed as a non-zero sideslip angle β during path following. The heading angle ψ relates the course angle χ according to: $\chi = \psi + \beta$. Vehicles can be controlled using a *course autopilot* if the course over ground (COG) is measured for instance using a global navigation satellite system (GNSS). However, for ships and underwater vehicles it is common to navigate using a *heading autopilot* with feedback from the yaw angle, which can be measured using a compass. In such cases it is of great interest to estimate the sideslip angle β to obtain accurate path-following control, that is regulate y_e to zero exponentially. The sideslip angle is quite small under normal operation of aircraft and marine craft. In fact only a few degrees of sideslip is observed during normal operation.

C. Parametrization of the sideslip angle

The main idea of this paper is to derive an adaptive integral LOS path-following control system to estimate β by treating β as an unknown constant parameter. This gives a *proportional-integral* guidance law. Furthermore, we will use adaptive control theory to prove stability and convergence of the integral term.

Assumption 1: The sideslip angle β is small and constant during path following such that $\dot{\beta} = 0$.

Remark 1: The sideslip angle is constant for straight lines and circular paths, which are used to construct *Dubins paths* [10]. The switching between the segments will appear as steps in the parameter update law. For vehicles traversing a non-circular feasible path (i.e. a small curvature path) β will be slowly varying. The dynamics of β will, however, be much slower than the control bandwidth and thus the adaptation law will track the changes. Also note that although the sideslip angle is relatively small (typically less than 5°), it largely affects the path-following properties of the vehicle, and if not properly compensated, this results in significant deviations from the desired path.

Consider (14) in the following form:

$$\begin{aligned} \dot{y}_e &= U\sin(\psi - \gamma_p + \beta) \\ &= U\sin(\psi - \gamma_p)\cos\beta + U\cos(\psi - \gamma_p)\sin\beta \end{aligned} \tag{15}$$

Assumption 1 implies that $\cos(\beta) \approx 1$ and $\sin(\beta) \approx \beta$, and thus (15) becomes:

$$\dot{y}_e = U\sin(\psi - \gamma_p) + U\cos(\psi - \gamma_p)\beta \tag{16}$$

III. LOS GUIDANCE ALGORITHMS

The LOS algorithms for path following are usually employed at a kinematic level where the goal is to prescribe a desired value for the heading angle ψ in (14). Consequently, the following assumption is employed:

Assumption 2: The heading autopilot tracks the desired heading angle perfectly such that $\psi = \psi_d$.

Remark 2: It is possible to relax Assumption 2 by analyzing a cascaded system where the second system includes the vehicle and autopilot dynamics by following the approach of Fredriksen and Pettersen [13]. The analysis of the total system is highly vehicle-dependent so the main result (Theorem 1) is limited to analyze the error dynamics at a kinematic level to give design flexibility with respect to different vehicles and autopilot systems.

A. Proportional LOS guidance

Since, the path tangential angle γ_p is known and the cross-track error y_e is measured, we choose:

$$\psi_d = \gamma_p + \tan^{-1}\left(-\frac{1}{\Delta}(y_e+\alpha)\right) \tag{17}$$

where $0 < \Delta_{\min} \leq \Delta \leq \Delta_{\max}$ is the user specified look-ahead distance and α is a control input to be designed later. The stability analysis of (14) with (17) makes use of:

$$\sin\left(\tan^{-1}\left(-\frac{1}{\Delta}(y_e+\alpha)\right)\right) = -\frac{y_e+\alpha}{\sqrt{\Delta^2+(y_e+\alpha)^2}} \tag{18}$$

$$\cos\left(\tan^{-1}\left(-\frac{1}{\Delta}(y_e+\alpha)\right)\right) = \frac{\Delta}{\sqrt{\Delta^2+(y_e+\alpha)^2}} \tag{19}$$

Substituting (18)–(19) into (16) under Assumptions 1 and 2 gives:

$$\dot{y}_e = -\frac{U(y_e+\alpha)}{\sqrt{\Delta^2+(y_e+\alpha)^2}} + \frac{U\Delta}{\sqrt{\Delta^2+(y_e+\alpha)^2}}\beta \tag{20}$$

If the sideslip angle is perfectly known, we can choose α to cancel the second term in (20). In particular, $\alpha = \Delta\beta$ gives

$$\dot{y}_e = -\frac{U}{\sqrt{\Delta^2+(y_e+\alpha)^2}}y_e \tag{21}$$

The stability properties of (21) are given by Proposition 1:

Proposition 1 (Proportional LOS guidance law with known sideslip angle): The equilibrium point $y_e = 0$ of the system (21) with $\alpha = \Delta\beta$ is USGES if $0 < \Delta_{\min} \leq \Delta \leq \Delta_{\max}$ and $0 < U_{\min} \leq U \leq U_{\max}$.

Proof: The system (21) is nonautonomous since U, α and Δ are time dependent. Consider the Lyapunov function candidate $V_1(t, y_e) = (1/2)y_e^2 > 0$ for all $y_e \neq 0$. Hence,

$$\dot{V}_1(t,y_e) = -\frac{U}{\sqrt{\Delta^2+(y_e+\alpha)^2}}y_e^2 \leq 0 \tag{22}$$

Since $V_1(t, y_e) > 0$ and $\dot{V}_1(t, y_e) \leq 0$ it follows that:

$$|y_e(t)| \leq |y_e(t_0)|, \quad \forall t \geq t_0 \tag{23}$$

Next, we define:

$$\phi^*(t,y_e) := \frac{U}{\sqrt{\Delta^2+(y_e+\alpha)^2}} \tag{24}$$

For each $r > 0$ and all $|y_e(t)| \leq r$, we have

$$\phi^*(t,y_e) \geq \frac{U_{\min}}{\sqrt{\Delta_{\max}^2+\left(r+\Delta_{\max}|\beta|\right)^2}} := c^*(r) \tag{25}$$

Consequently,

$$\begin{aligned}\dot{V}_1(t,y_e) &= -2\phi^*(t,y_e)V_1(t,y_e) \\ &\leq -2c^*(r)V_1(t,y_e), \qquad \forall |y_e(t)| \leq r\end{aligned} \tag{26}$$

In view of (23), the above holds for all trajectories generated by the initial conditions $y_e(t_0)$. Consequently, we can invoke the comparison lemma (Khalil [16], Lemma 3.4) by noticing that the linear system $\dot{w} = -2c^*(r)w$ has the solution $w(t) = e^{-2c^*(r)(t-t_0)}w(t_0)$, which implies that $\dot{v}_1(t) \leq e^{-2c^*(r)(t-t_0)}v_1(t_0)$ for $v_1(t) = V_1(t, y_e(t))$. Therefore,

$$y_e(t) \leq e^{-c^*(r)(t-t_0)}y_e(t_0) \tag{27}$$

for all $t \geq t_0$, $|y_e(t_0)| \leq r$ and any $r > 0$. Hence, we can conclude that the equilibrium point $y_e = 0$ is USGES (Loria and Panteley [20], Definition 2.7). ■

Remark 3: Notice that global exponential stability (GES) cannot be achieved due to the structural properties of the cross-track error dynamics (14), which contains a sinusoidal function introducing saturation. This is the reason why the system gain in (21) decreases with the magnitude of the cross-track error and thus global exponential convergence cannot be achieved.

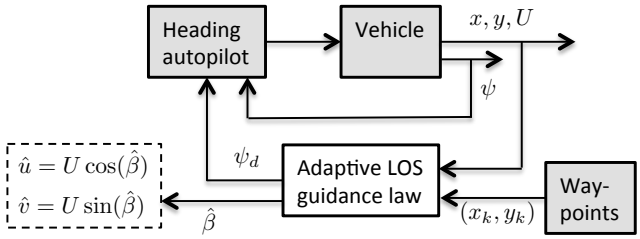

Fig. 2. The adaptive integral LOS guidance law as reference generator to a commercial autopilot system. The estimated sideslip angle $\hat{\beta}$ also gives estimates $\hat{u}$ and $\hat{v}$ of the surge and sway velocities, respectively.

B. Adaptive compensation of the sideslip angle

Let $\hat{\beta}$ denote the adaptive estimate of β and $\tilde{\beta} = \beta - \hat{\beta}$ the parameter estimation error. An adaptive controller can be designed such that the input $\alpha = \Delta\hat{\beta}$ cancels the sideslip angle β in (20). The main result is summarized in Theorem 1.

Theorem 1 (Adaptive integral LOS guidance law): Under Assumptions 1 and 2, the adaptive integral LOS guidance law:

$$\psi_d = \gamma_p + \tan^{-1}\left(-\frac{1}{\Delta}y_e - \hat{\beta}\right) \tag{28}$$

$$\dot{\hat{\beta}} = \gamma\frac{U\Delta}{\sqrt{\Delta^2+(y_e+\Delta\hat{\beta})^2}}y_e, \quad \gamma > 0 \tag{29}$$

applied to (16) with $0 < \Delta_{\min} \leq \Delta \leq \Delta_{\max}$ and $0 < U_{\min} \leq U \leq U_{\max}$ renders the origin $(y_e, \tilde{\beta}) = (0, 0)$ USGES.

Proof: Equation (20) with $\alpha = \Delta\hat{\beta}$ becomes:

$$\dot{y}_e = -\frac{U}{\sqrt{\Delta^2+(y_e+\Delta\hat{\beta})^2}}y_e + \frac{U\Delta}{\sqrt{\Delta^2+(y_e+\Delta\hat{\beta})^2}}\tilde{\beta} \tag{30}$$

Notice that cross-track error dynamics is nonautonomous since both U and Δ can be time-varying. Consider:

$$V_2(t,y_e,\tilde{\beta}) = \frac{1}{2}y_e^2 + \frac{1}{2\gamma}\tilde{\beta}^2 > 0, \quad y_e \neq 0, \tilde{\beta} \neq 0 \tag{31}$$

with $\gamma > 0$. From (30) and (31) it follows that:

$$\begin{aligned}\dot{V}_2(t,y_e,\tilde{\beta}) = &-\frac{U}{\sqrt{\Delta^2+(y_e+\Delta\hat{\beta})^2}}y_e^2 \\ &+ \tilde{\beta}\left(\frac{U\Delta}{\sqrt{\Delta^2+(y_e+\Delta\hat{\beta})^2}}y_e + \frac{1}{\gamma}\dot{\tilde{\beta}}\right)\end{aligned} \tag{32}$$

Since $\dot{\tilde{\beta}} = -\dot{\hat{\beta}}$, we can substitute (29) into (32). This gives:

$$\dot{V}_2(t, y_e, \tilde{\beta}) = -\frac{U}{\sqrt{\Delta^2 + (y_e + \Delta\hat{\beta})^2}} y_e^2 \leq 0 \tag{33}$$

Since $V_2(t, y_e, \tilde{\beta}) > 0$ and $\dot{V}_2(t, y_e, \tilde{\beta}) \leq 0$ it follows that

$$|y_e(t)| \leq |y_e(t_0)|, \;\; |\tilde{\beta}(t)| \leq |\tilde{\beta}(t_0)| \quad \forall t \geq t_0 \tag{34}$$

Next, we define $x = [x_1, x_2]^\top := [y_e, \tilde{\beta}]^\top$ such that:

$$\bar{\phi}(t, x) := \frac{U}{\sqrt{\Delta^2 + (x_1 + \Delta(\beta - x_2))^2}} \tag{35}$$

For each $\bar{r} > 0$ and all $\|x(t)\| \leq \bar{r}$, we have

$$\bar{\phi}(t, x) \geq \frac{U_{\min}}{\sqrt{\Delta_{\max}^2 + \left(\max\{1, \Delta_{\max}\}\bar{r} + \Delta_{\max}|\beta|\right)^2}} := c(\bar{r}) \tag{36}$$

From (29) and (30) it follows that:

$$\dot{x}_1 = -\bar{\phi}(t, x)x_1 + \Delta\bar{\phi}(t, x)x_2 \tag{37}$$

$$\dot{x}_2 = -\gamma\Delta\bar{\phi}(t, x)x_1 \tag{38}$$

In order to prove USGES we make use of:

$$V_3(t, x) = \frac{1}{2}x_1^2 + \frac{1}{2\gamma}x_2^2 - \varepsilon x_1 x_2 := \frac{1}{2}x^\top P x \tag{39}$$

where $0 < \varepsilon < 1/\sqrt{\gamma}$ such that

$$P = \begin{bmatrix} 1 & -\varepsilon \\ -\varepsilon & 1/\gamma \end{bmatrix} > 0 \tag{40}$$

Consequently,

$$\begin{aligned} \dot{V}_3(t, x) = {} & x_1\left(-\bar{\phi}(t, x)x_1 + \Delta\bar{\phi}(t, x)x_2\right) \\ & + \frac{1}{\gamma}x_2\left(-\gamma\Delta\bar{\phi}(t, x)x_1\right) \\ & - \varepsilon x_2\left(-\bar{\phi}(t, x)x_1 + \Delta\bar{\phi}(t, x)x_2\right) \\ & - \varepsilon x_1\left(-\gamma\Delta\bar{\phi}(t, x)x_1\right) \end{aligned} \tag{41}$$

From this it follows that:

$$\begin{aligned} \dot{V}_3(t, x) &= -\bar{\phi}(t, x)\left((1 - \varepsilon\gamma\Delta)\, x_1^2 + \varepsilon\Delta x_2^2 - \varepsilon x_1 x_2\right) \\ &\leq -2c(\bar{r})x^\top Q(t)x \end{aligned} \tag{42}$$

where

$$Q(t) = \begin{bmatrix} 1 - \varepsilon\gamma\Delta(t) & -\frac{\varepsilon}{2} \\ -\frac{\varepsilon}{2} & \varepsilon\Delta(t) \end{bmatrix} \tag{43}$$

The matrix $Q(t)$ is time varying but $0 < \Delta_{\min} \leq \Delta(t) \leq \Delta_{\max}$ for all $t \geq 0$. Hence, there exists a positive constant ε:

$$0 < \varepsilon < \min\left\{\frac{1}{\sqrt{\gamma}}, \frac{1}{\gamma\Delta_{\max}}, \frac{4\Delta_{\min}}{4\gamma\Delta_{\max}^2 + 1}\right\} \tag{44}$$

for any $\gamma > 0$ guaranteeing that

$$\dot{V}_3 \leq -2\frac{q_{\min}}{p_{\max}}c(\bar{r})V_3, \quad \forall \|x(t)\| \leq \bar{r} \tag{45}$$

where $p_{\max} = \max\{1, 1/\gamma\}$ and $q_{\min} = \lambda_{\min}(Q)$. In view of (34), the above holds for all trajectories generated by the initial conditions $x(t_0)$. Hence, we can invoke the comparison lemma (Khalil [16], Lemma 3.4) by noticing that the linear system $\dot{w} = -2(q_{\min}/p_{\max})c(\bar{r})w$ has the solution $w(t) = e^{-2(q_{\min}/p_{\max})c(\bar{r})(t-t_0)}w(t_0)$, which implies that $v_3(t) \leq e^{-2(q_{\min}/p_{\max})c(\bar{r})(t-t_0)}v_3(t_0)$ for $v_3(t) = V_3(t, x(t))$. Hence, defining $p_{\min} = \min\{1, 1/\gamma\}$ it follows that:

$$\|x(t)\| \leq \sqrt{\frac{p_{\max}}{p_{\min}}}e^{-\frac{q_{\min}}{p_{\max}}c(\bar{r})(t-t_0)}\|x(t_0)\| \tag{46}$$

for all $t \geq t_0$, $\|x(t_0)\| \leq \bar{r}$ and any $\bar{r} > 0$. Hence, we can conclude that the equilibrium point $x = 0$ is USGES (Loria and Panteley [20], Definition 2.7).

■

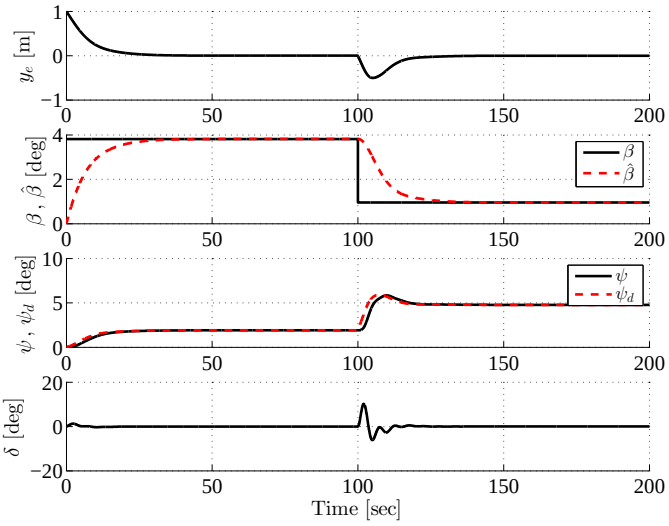

Fig. 3. Straight-line path following. The plots show the cross-track error y_e, estimated sideslip angle $\hat{\beta}$, desired and actual heading angle ψ_d and ψ, respectively, and rudder angle δ.

IV. Case Studies

A. Straight-line path following: Ship exposed to steps in sideslip angle

In order to demonstrate the exponential convergence properties of the adaptive integral LOS guidance law given by Theorem 1 we first consider straight-line path following. The path-tangential angle is chosen as $\gamma_p = (180/\pi)\cdot 0.1 \approx 5.73°$. The control law was implemented using $\Delta = 10$ m and $\gamma = 0.003$. The ship yaw dynamics was chosen as a first-order *Nomoto model* with actuator dynamics (Fossen [12]):

$$T\ddot{\psi} + \dot{\psi} = K\delta \tag{47}$$

$$\dot{\delta} = \frac{1}{T_\delta}(\delta_c - \delta) \tag{48}$$

with $T_\delta = 1$ s, $T = 20$ s and $K = 1$ rad/s. The rudder angle command δ_c is generated using a heading autopilot of PD type:

$$\delta_c = -K_p(\psi - \psi_d) - K_d\dot{\psi} \tag{49}$$

where K_p and K_d were chosen to give a critically damped system with natural frequency 1 rad/s. We consider two scenarios:

S1 The surge and sway velocities are initially chosen as $u = 3.0$ m/s and $v = 0.2$ m/s. This corresponds to a sideslip angle of $\beta \approx 3.81°$.

S2 After 100 seconds the sway velocity is changed to $v = 0.05$ m/s corresponding to $\beta \approx 0.95°$.

The transition from Scenario S1 to S2 is observed as a step in Figure 3. Nevertheless, the estimated sideslip angle converges to its true value. The cross-track error is also converging to zero as stated by Theorem 1. Even though the heading autopilot does not include reference feedforward excellent performance is demonstrated for step inputs in velocity and sideslip angle.

B. Curved-path path following: Ship exposed to time-varying ocean currents

The robustness of the adaptive integral LOS guidance law is further tested on a 4-DOFs maneuvering model (surge-sway-roll-yaw) of a *multirole naval vessel* (Blanke and Christensen [3]), which follows a curved path while being subject to the action of an irrotational ocean current.

Let $\boldsymbol{\eta} = [N, E, \phi, \psi]^\top$ and $\boldsymbol{\nu} = [u, v, p, r]^\top$ be the generalized position and velocity vectors, respectively. The North-East position is denoted as (N, E), ϕ is the roll angle and ψ is the heading angle. The equations of motion read:

$$\dot{\boldsymbol{\eta}} = \mathbf{J}(\boldsymbol{\eta})\boldsymbol{\nu} \tag{50}$$

$$\mathbf{M}\dot{\boldsymbol{\nu}} + \mathbf{C}_{RB}(\boldsymbol{\nu})\boldsymbol{\nu} + \mathbf{N}(\boldsymbol{\nu}_r)\boldsymbol{\nu}_r + \mathbf{g}(\boldsymbol{\eta}) = \boldsymbol{\tau}_c \tag{51}$$

where $\mathbf{J}(\boldsymbol{\eta})$ is a coordinate transformation; $\mathbf{M}$ is the mass matrix including rigid-body inertia and hydrodynamic added inertia terms; $\mathbf{C}_{RB}(\boldsymbol{\nu})$ is the rigid-body Coriolis and centripetal forces/moments matrix; $\boldsymbol{\nu}_r = \boldsymbol{\nu} - \boldsymbol{\nu}_c$ is the relative vessel velocity given by the difference between the generalized velocity vector and the current velocity vector $\boldsymbol{\nu}_c = [u_c, v_c, 0, 0]^\top$ expressed in body coordinates; $\mathbf{N}(\boldsymbol{\nu}_r) = \mathbf{C}_A(\boldsymbol{\nu}_r) + \mathbf{D}(\boldsymbol{\nu}_r)$ is the matrix collecting the added mass Coriolis and centripetal terms together with the hydrodynamic damping; $\mathbf{g}(\boldsymbol{\eta})$ is the vector of restoring forces/moments; $\boldsymbol{\tau}_c = [\tau_u, \tau_v, \tau_\phi, \tau_\psi]^\top$ is the vector of control forces and moments generated by the propulsion system and the rudder deflection. The numerical values of the parameters of this model can be found in Blanke and Christensen [3].

The propeller thrust is kept at the constant value $\tau_u = 115.75\,\mathrm{kN}$, which corresponds to a constant speed $U \approx 7.7\,\mathrm{m/s}$ in calm waters. A heading autopilot of PID type:

$$\delta_c = -K_p(\psi - \psi_d) - K_i \int_{t_0}^{t} (\psi - \psi_d)\,\mathrm{d}\tau - K_d\dot{\psi} \tag{52}$$

is used to generate the commanded rudder deflection. The controller gains K_p, K_i and K_d were selected to obtain a closed-loop steering dynamics with a damping ratio $\zeta_s = 0.95$ and a bandwidth $\omega_s \approx 0.42\,\mathrm{rad/s}$.

Note that the integral action provided by (29) yields an integral effect for the cross-track error y_e given by (30). This ensures that $\tilde{\beta}$ goes to zero in the presence of environmental disturbances while the integral term in the autopilot (52) is necessary for the heading error $\psi - \psi_d$ to converge to zero. In particular, sideslipping due to slowly varying ocean currents, waves and wind forces is handled by the integral term (29), which computes the correct ψ_d for path following in the presence of environmental disturbances. The integral term in (52), however, cancels the rudder bias of the steering machine and compensates for unmodeled dynamics in the autopilot.

The PID controller (52) sends the command to the rudder machinery, which executes it according to:

$$\dot{\delta}_e = \mathrm{sat}\left(\frac{1}{T_\delta}(\mathrm{sat}(\delta_c) - \delta_e)\right) \tag{53}$$

$$y_\delta = \delta_e + \delta_0 \tag{54}$$

where $\mathrm{sat}(\cdot)$ is the saturation function, $T_\delta = 0.2\,\mathrm{s}$ is the rudder time constant and δ_0 is the rudder bias.

The irrotational ocean current speed V_c is generated as the sum of a constant term and a stochastic term, whereas the current direction β_c is constant in the inertial coordinate system. Hence, the body-fixed current velocities becomes:

$$u_c = V_c\cos(\beta_c - \psi), \quad v_c = V_c\sin(\beta_c - \psi) \tag{55}$$

For more details about modeling of ocean currents the reader is addressed to Chapter 8.3 in Fossen [12].

The vessel travels along a curved path between the starting pose $P_0 = (N_0, E_0, \psi_0)$ and the end pose $P_1 = (N_1, E_1, \psi_1)$. The path shown in Figure 4 is represented by the interconnection of two straight lines with a circle arc, which is motivated by construction of so-called Dubins paths [10] representing the shortest distance between two poses P_0 and P_1 when traveling at constant speed. The adaptive integral LOS guidance law is then tested on two scenarios:

S1 At time $t = 700\,\mathrm{s}$ a current with speed $V_c = 0.3\,\mathrm{m/s}$ and direction $\beta_c = 30°$ starts affecting the vessel. Only the deterministic part of the current is considered. The rudder bias δ_0 is set equal to zero.

S2 For $0 \leq t < 700\,\mathrm{s}$ a stochastic current with speed $V_c = 0.3\,\mathrm{m/s}$ and direction $\beta_c = -20°$ affects the vessel, whereas for $t \geq 700\,\mathrm{s}$ the current speed decreases to $V_c = 0.25\,\mathrm{m/s}$ and the direction changes to $\beta_c = 30°$. The stochastic component of the current has a variance $\sigma^2_{V_c} = 0.01\,\mathrm{m^2/s^2}$. Moreover, the rudder bias is set equal to $\delta_0 = 5°$.

In both scenarios the adaptive integral LOS guidance law is implemented with a look-ahead distance $\Delta = 100\,\mathrm{m}$ and an adaptation gain $\gamma = 3 \cdot 10^{-5}$.

Figures 5 and 6 show the performance of the adaptive LOS guidance law in connection with the heading autopilot when tested on S1. When the sideslip angle is constant the proposed adaptive LOS guidance law provides a perfect estimate of it in agreement with Theorem 1. This is clearly visible in Fig. 5 both when the vessel is in the first half of the turning maneuver ($400\,\mathrm{s} < t \leq 700\,\mathrm{s}$) and when the vessel is following the last part of the straight path while being subject to the constant current ($t \geq 1100\,\mathrm{s}$). In the time interval $700\,\mathrm{s} \leq t < 1100\,\mathrm{s}$ the sideslip angle β is given by the sum of two contributions:

- A term that depends on the path curvature (zero for straight lines and constant for circular paths).
- A time-varying term due to the action of the current whose magnitude in the body-fixed frame changes in relation to the heading angle ψ.

Although the adaptive integral LOS guidance law is not designed for tracking a time-varying sideslip angle, it is worth

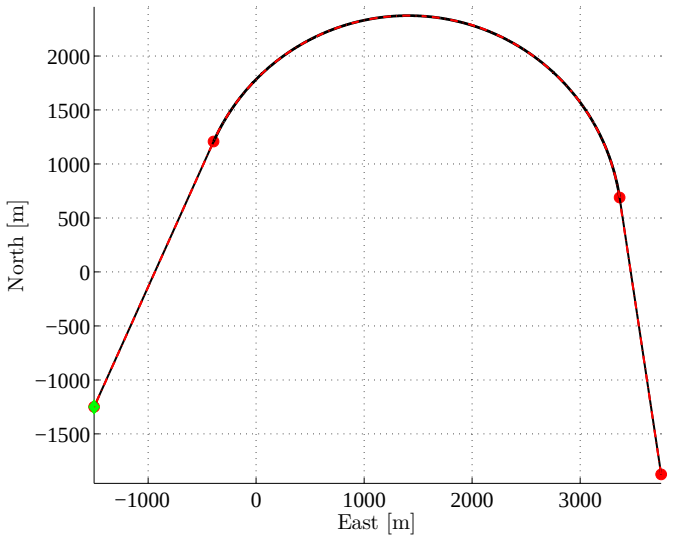

Fig. 4. Curved-path path following. The plot shows the superposition of the curved path to be followed (black solid line) and the actual path traveled by the vessel (red dashed line). The starting pose P_0 is given by the green diamond.

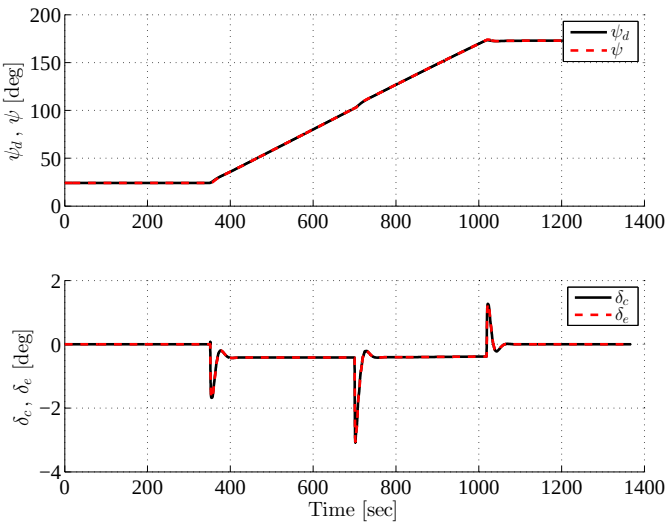

Fig. 6. Curved-path path following. The plots show the desired and actual heading angle ψ_d and ψ, and the commanded and executed rudder angle δ_c and δ_e.

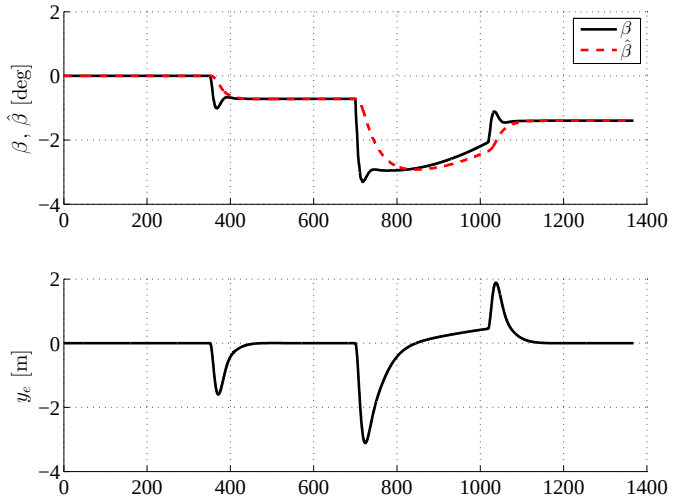

Fig. 5. Curved-path path following. The plots show the estimated sideslip angle $\hat{\beta}$ in comparison to the true β, and the cross-track error y_e.

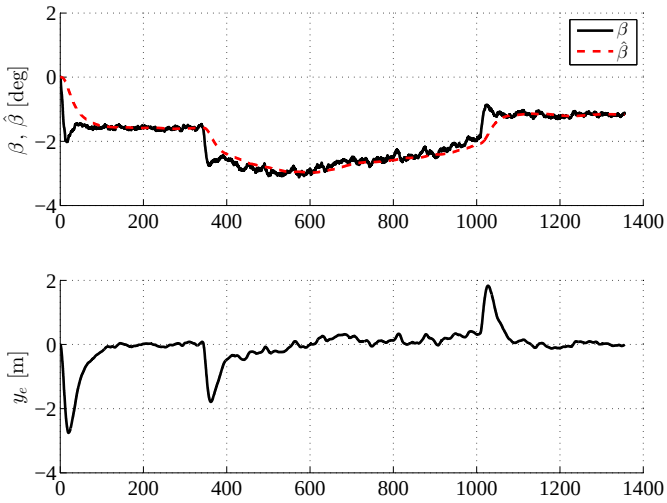

Fig. 7. Curved-path path following while being subject to a stochastic current. The plots show the estimated sideslip angle $\hat{\beta}$ in comparison to the true β, and the cross-track error y_e.

noting that the estimate $\hat{\beta}$ closely follows the behavior of the true sideslip angle.

It is also interesting to observe the good synergy between the integral action of the adaptive LOS guidance law (29) and the integral action of the heading autopilot (52). This is clearly evident by looking at the time history of the executed rudder deflection δ_e in Fig. 6 in connection with the time history of the estimated sideslip angle $\hat{\beta}$ in Fig. 5 for time $t \geq 1100\,\mathrm{s}$. Once the vessel has finished the turning maneuver the rudder position goes back to zero and the sideslip angle due to the current is completely compensated at kinematic level by the adaptive integral LOS guidance law.

Deviations of the cross-track error y_e from zero in correspondence of the beginning and the end of the turning maneuver are expected. In fact when the curvature of the path changes the vessel does not have yet a turning rate different from zero that would allow for the instantaneous following of the path. The rudder takes approximately 20 seconds to move to the new position, and it is only after this time that the vessel has the turning rate to correctly follow the path.

Figures 7 and 8 show the performance of the proposed adaptive integral LOS guidance law in connection with the heading autopilot when tested on S2. The addition of the stochastic component in the ocean current speed does not deteriorate the overall performance. The estimate $\hat{\beta}$ well follows the mean value of the true sideslip angle throughout the entire path, and the cross-track error y_e is kept fluctuating about zero. Moreover the rudder bias δ_0 is compensated by the integral action of the heading autopilot, and it does not

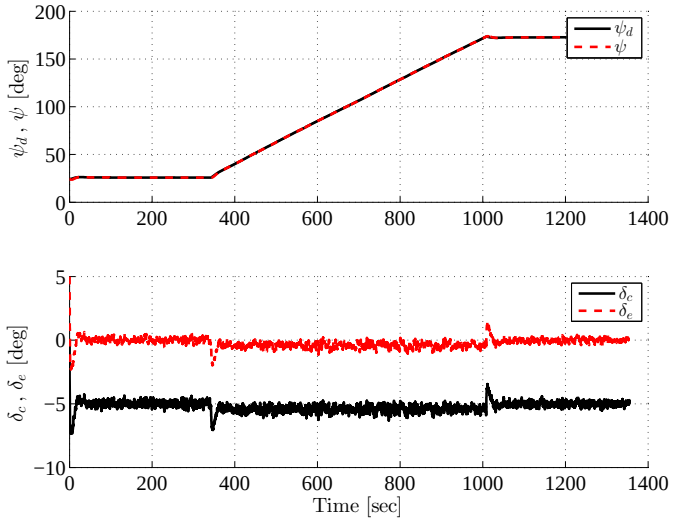

Fig. 8. Curved-path path following while being subject to a stochastic current. The plots show the desired and actual heading angle ψ_d and ψ, and the commanded and executed rudder angle δ_c and δ_e.

affect the performance of the adaptive LOS guidance law.

V. Conclusions

A nonlinear adaptive path-following algorithm for estimation and compensation of the sideslip angle has been presented. This allows for effective compensation of vehicle sideslip, which is caused by wind, waves and ocean currents.

The equilibrium points of the cross-track and parameter estimation errors are shown to be uniformly semiglobally exponentially stable (USGES). This guarantees that the estimated sideslip angle converges exponentially to its true value for paths with constant curvature. The adaptive guidance law is based on a classical LOS guidance principle for marine craft and integral action is obtained by parameter adaptation. The proposed *integral LOS guidance law* uses the cross-track error and path-tangential angle to obtain path following. The path is assumed to be a parametrized curve.

Computer simulations, where straight lines and circle arcs are combined to form a so-called Dubins path, are used to verify that it is possible to estimate the sideslip angle during vehicle path following in presence of unknown environmental disturbances.

Acknowledgment

T. I. Fossen was supported by Otto Mønsted foundation when he was visiting professor at the Technical University of Denmark in 2013. The work was also supported by the Norwegian Research Council (project no. 223254) through the Center for Autonomous Marine Operations and Systems (AMOS) at the Norwegian University of Science and Technology.

References

[1] A. P. Aguiar and J. P. Hespanha. Trajectory-tracking and path-following of underactuated autonomous vehicles with parametric modeling uncertainty. *IEEE Trans. on Automatic Control*, Vol. 52, No. 8, 2007, pp. 1362–1379.

[2] M. Aicardi, G. Casalino, G. Indiveri, A. Aguiar, P. Encarnaçao and A. Pascoal. A planar path following controller for underactuated marine vehicles. In: *Proc. 9th Mediterranean Conf. on Control and Automation*, 2001.

[3] M. Blanke and A. Christensen. Rudder roll damping autopilot robustness to sway-yaw-roll coupling. In: *Proc. 10th SCSS*, Ottawa, Canada, 1993.

[4] M. Breivik, V. E. Hovstein and T. I. Fossen. Straight-line target tracking for unmanned surface vehicles. *Modeling, Identification and Control*, vol. 29, no. 4, 2008, pp. 131–149.

[5] M. Breivik and T. I. Fossen. *Guidance laws for autonomous underwater vehicles*. In: *"Intelligent Underwater Vehicles"*. I-Tech Education and Publishing (A. V. Inzartsev, Ed.), Ch. 4, pp. 51–76, Vienna, 2009.

[6] E. Børhaug and K. Y. Pettersen. Cross-track control for underactuated autonomous vehicles. In: *Proc. IEEE Conference on Decision and Control*, Seville, Spain, 2005, pp. 602–608.

[7] E. Børhaug and K. Y. Pettersen. LOS path following for underactuated underwater vehicles. In: *Proc. IFAC Conference on Maneouvring and Control of Marine Craft*, Lisbon, Portugal, 2006.

[8] E. Børhaug, A. Pavlov and K. Y. Pettersen. Integral LOS control for path following of underactuated marine surface vessels in the presence of constant ocean currents. In: *Proc. IEEE Conference on Decision and Control*, Cancun, Mexico, 2008, pp. 4984–4991.

[9] K. D. Do, Z.-P. Jiang and J. Pan. Robust adaptive path following of underactuated ships, *Automatica*, Vol. 40, No. 6, 2004, pp. 929–944.

[10] L. Dubins. On curves of minimal length with a constraint on average curvature and with prescribed initial and terminal positions and tangents. *American Journal of Mathematics*, Vol. 79, pp. 497–516, 1957.

[11] T. I. Fossen, M. Breivik and R. Skjetne. Line-of-sight path following of underactuated marine craft. In: *Proc. IFAC Conference on Maneouvring and Control of Marine Craft*, Girona, Spain, 2003, pp. 244-249.

[12] T. I. Fossen. *Handbook of Marine Craft Hydrodynamics and Motion Control*. Wiley, 2011.

[13] E. Fredriksen and K. Y. Pettersen. Global κ-exponential waypoint maneuvering of ships: theory and experiments. *Automatica*, Vol. 42, No. 4, 2006, pp. 677–687.

[14] F. Hao, R. Lenain, B. Thuilot and P. Martinet. Robust adaptive control of automatic guidance of farm vehicles in the presence of sliding. In: Proc. IEEE Conf. on Robotics and Automation (ICRA), 2005.

[15] A. J. Healey and D. Lienard. Multivariable sliding mode control for autonomous diving and steering of unmanned underwater vehicles. *IEEE Journal of Oceanic Engineering*, vol. 18, no. 3, 1993, pp. 327–339.

[16] H. K. Khalil. *Nonlinear Systems*. Prentice-Hall. 2002.

[17] L. Lapierre, D. Soetanto and A. Pascoal. Nonlinear path following with applications to the control of autonomous underwater vehicles. In: *Proc. 42nd IEEE Conf. on Decision and Control*, Vol. 2, 2003, pp. 1256–1261.

[18] A. M. Lekkas and T. I. Fossen. Line-of-sight guidance for path following of marine vehicles. Chapter 5. In: *Advanced in Marine Robotics*, LAP LAMBERT Academic Publishing (O. Gal, Ed.), 2013, pp. 63–92.

[19] R. Lenain, B. Thuilot, C. Cariou and P. Martinet. High accuracy path tracking for vehicles in presence of sliding: Application to farm vehicle automatic guidance for agricultural tasks. *Autonomous robots*, 2006.

[20] A. Loria and E. Panteley. Cascaded nonlinear time-varying systems: analysis and design. Ch. 2. In: *Advanced Topics in Control Systems Theory*, Springer-Verlag London (F. Lamnabhi-Lagarrigue, A. Loria and E. Panteley Eds.), 2004, pp. 23–64.

[21] K. Y. Pettersen and E. Lefeber. Waypoint tracking control of ships. In: *Proc. IEEE Conference on Decision and Control*, Orlando, Florida, 2001, pp. 940–945.

[22] C. Samson. Path following and time-varying feedback stabilization of a wheeled mobile robot. In: *Proc. Int. Conf. ICARCV'92*, 1992.

[23] P. Morin and C. Samson. Motion control of wheeled mobile robots. Ch. 34 in the *"Springer Handbook of Robotics"* (B. Sicilliano and O. Khatib, Eds.), Springer, 2008.

[24] R. Skjetne, T. I. Fossen and P. V. Kokotovic. Robust output maneuvering for a class of nonlinear systems. *Automatica*, vol. 40, no. 3, 2004, pp. 373-383.

[25] G. M. Siouris. *Missile Guidance and Control Systems*, Springer, 2010.

[26] O. J. Sørdalen and O. Egeland. Exponential stabilization of nonholonomic chained systems. *IEEE Transactions on Automatic Control*, Vol. 40, No. 1, 1995.

[27] R. Yanushevsky. *Guidance of Unmanned Aerial Vehicles*. CRC Press, 2011.